We are IntechOpen,
the world's leading publisher of
Open Access books
Built by scientists, for scientists

6,900
Open access books available

185,000
International authors and editors

200M
Downloads

Our authors are among the

154
Countries delivered to

TOP 1%
most cited scientists

12.2%
Contributors from top 500 universities

CLARIVATE ANALYTICS
BOOK CITATION INDEX
INDEXED

WEB OF SCIENCE™

Selection of our books indexed in the Book Citation Index
in Web of Science™ Core Collection (BKCI)

Interested in publishing with us?
Contact book.department@intechopen.com

Numbers displayed above are based on latest data collected.
For more information visit www.intechopen.com

Shapiro Steps in BSCCO Intrinsic Josephson Junctions

Michihide Kitamura

Department of Electrical and Electronic System Engineering, Utsunomiya University,
Yoto, Utsunomiya, Tochigi
Japan

1. Introduction

In 1963, Shapiro did an experiment for the microwave irradiation effect on the *I-V* characteristics of a Josephson junction $Al/Al_2O_3/Sn$ and showed that when the microwave is impressed to the Josephson junction, clear current steps are observed on the quasiparticle (QP) branches of the *I-V* characteristics and those steps, which are now called "Shapiro steps", are observed on constant voltages given by $n\Phi_0 f_r$ ($n = \pm 1, \pm 2, ...$) [1]. Here the Φ_0 is a flux quantum ($= 2.06785 \times 10^{-15}$ Wb) defined by $h/2e$ using Planck constant h and the f_r is the frequency of the impressed microwave. The interactions between the Josephson junction and the electromagnetic field are important and intersting problems on not only the fundamental but also the applicational points of view. The Shapiro steps are one of the important phenomena observed on a superconductor-insulator-superconductor (SIS)-type Josephson junction.

It is well known that the high-T_c superconductors such as $Bi_2Sr_2CaCu_2O_{8+\delta}$ (BSCCO) and $(Pb_yBi_{1-y})_2Sr_2CaCu_2O_{8+\delta}$ (PBSCCO) consist of a stack of atomic-scale Josephson junctions called intrinsic Josephson junctions (IJJs) and these IJJs are SIS-type Josephson junctions. [2– 8] The stacking structure of IJJs along the crystallographic *c*-axis can be made *naturally*, so that these natural super-lattices can be regarded as a stack of good quality Josephson devices made under the atomic-scale. This is just a reason why the studies of the current flow along the *c*-axis have been done extensively for the high-T_c superconductors. It has been already established that the high-T_c superconductors such as BSCCO and PBSCCO are characterized by the $d_{x^2-y^2}$-symmetry superconducting gap rather than the *s*-one. [9–11] There are some excellent works for Shapiro steps on BSCCO single crystals. [12–18]

When a *large* SIS Josephson junction is embedded in the magnetic field applied parallel to the junction surface, the fluxon dynamics in the SIS Josephson junction can be understood by solving a following nonlinear partial differential equation. [19]

$$\frac{\partial^2 \varphi}{\partial x^2} - \frac{1}{\bar{c}^2}\frac{\partial^2 \varphi}{\partial t^2} - \frac{\beta}{\bar{c}^2}\frac{\partial \varphi}{\partial t} = \frac{1}{\lambda_J^2}\sin\varphi \, , \tag{1}$$

where $\bar{c}$ is Swihart velocity, λ_J is Josephson penetration depth and φ is the phase difference of a SIS Josephson junction as a function of spacial variable x and real time t. As already stated,

BSCCO consists of a stack of SIS-type IJJs, so it is expected that the BSCCO should be regarded as a good sample to study the fluxon dynamics in the SIS Josephson junctions. Actually, there are many excellent works for the effect of magnetic field on the BSCCO IJJs. [20–34] It is sure that a pioneering work done by Sakai, Bodin and Pedersen(SBP) [20] is the starting point to understand the fluxon dynamics in BSCCO IJJs with a stacking structure.

We adopt here a unified theory proposed by Machida and Sakai (MS) [29], which includes both the electric and magnetic field couplings between neighboring IJJs in multistacked structure. The MS-unified theory is a further extension of the model proposed by Sakai, Bodin and Pedersen (SBP). [20] Present paper is mainly based on my previous jobs. [35, 36]

2. Theory

Let us consider a stacked system consisting of N-identical SIS-Josephson junctions such as IJJs in BSCCO high-T_c superconductors, and set spacial coodinates x, y and z parallel to a, b and c axes of a BSCCO single crystal. If the external magnetic induction $\mathbf{B}_{ext}$ is selected parallel to y-axis, i.e., $\mathbf{B}_{ext} = (0, B_{ext}, 0)$, and the spacial variation of the gauge-invariant phase difference φ_ℓ for the ℓ-th SIS Josephson junction is assumed as a function of only x, then the $\varphi_\ell(x, t)$ as a function of x and real time t satisfies a following coupled sine-Gordon(CSG) equation with a matrix form. [29]

$$\Sigma_{\mathbf{c}}\lambda_J^2 \frac{\partial^2}{\partial x^2} \begin{pmatrix} \varphi_1(x, t) \\ . \\ \varphi_\ell(x, t) \\ . \\ \varphi_N(x, t) \end{pmatrix} = \Sigma_{\mathbf{L}} \begin{pmatrix} \mathcal{J}_1(x, t) \\ . \\ \mathcal{J}_\ell(x, t) \\ . \\ \mathcal{J}_N(x, t) \end{pmatrix}, \tag{2}$$

where λ_J is the Josephson penetration depth given by $\sqrt{\Phi_0/2\pi\mu_0 d'_L J_c}$ using a flux quantum Φ_0, the vacuum permeability μ_0 and the critical current density J_c. The $\Sigma_{\mathbf{c}}$ and $\Sigma_{\mathbf{L}}$ are matrices describing the electric and magnetic interactions between neighboring Josephson junctions and are written as

$$\Sigma_{\mathbf{c(L)}} = \begin{pmatrix} 1 & \Sigma_{c(L)} & 0 & . & . \\ \Sigma_{c(L)} & 1 & \Sigma_{c(L)} & 0 & . \\ . & \Sigma_{c(L)} & 1 & \Sigma_{c(L)} & . \\ . & . & . & . & . \\ . & . & 0 & \Sigma_{c(L)} & 1 \end{pmatrix}, \tag{3}$$

where the coupling constants Σ_c and Σ_L are given by [29]

$$\Sigma_{c(L)} = -\frac{\lambda_{e(L)}}{d'_{c(L)} \sinh(w/\lambda_{e(L)})}. \tag{4}$$

The d'_c and d'_L are the effective electric and magnetic thickness given by [29]

$$d'_{c(L)} = d + 2\lambda_{e(L)} \coth(w/\lambda_{e(L)}), \tag{5}$$

using electrode thickness w and barrier thickness d. The λ_e and λ_L are the Debye screening length and the London penetration depth, respectively. The $\mathcal{J}_\ell(x, t)$ in Eq.(2) is the current defined by $j_J^{(\ell)}(x, t) - j_{ext}(t)$. The $j_J^{(\ell)}(x, t)$ and $j_{ext}(t)$ are junction and external currents

normalized to the critical current $I_c (= J_c S)$, therefore, the current $\mathcal{J}_\ell(x,t)$ can be written in SI units as

$$\mathcal{J}_\ell(x,t) = \left(\frac{\Phi_0}{2\pi}\right) \frac{C_u^*}{J_c} \frac{\partial^2 \varphi_\ell(x,t)}{\partial t^2} + \left(\frac{\Phi_0}{2\pi}\right) \frac{G_u^*}{J_c} \frac{\partial \varphi_\ell(x,t)}{\partial t} + \sum_{\ell'=1}^{N} \{\mathbf{\Sigma_c}\}_{\ell,\ell'} \, i_{CP}^{(\ell')}(x,t) - j_{ext}(t) \,, \quad (6)$$

where C_u^* and G_u^* are the effective unit area capacitance $\varepsilon \varepsilon_0 / d_c'$ and conductivity σ / d_c' per a junction, respectively. The current $i_{CP}^{(\ell)}(x,t)$ is the normalized Cooper-pair (CP) tunneling current of the ℓ-th SIS Josephson junction whose general form has been already presented in my previous paper. [35] Note that the simplest form of $i_{CP}^{(\ell)}(x,t)$ is $\sin \varphi_\ell(x,t)$. The external current $j_{ext}(t)$ is the same as the normalized external current $i_{ext}(t)$ presented in my previous paper, that is,

$$j_{ext}(t) = i_0 + i_r \sin \omega_r t + i_{noise}(t,T) \equiv j_{ext}(t,T) \,, \quad (7)$$

where i_0 is the normalized external dc, $i_r \sin \omega_r t$ is the normalized external ac modulation current with the frequency ω_r and $i_{noise}(t,T)$ is the normalized current due to thermal noise at a sample temperature T. As a noise, we consider here a "white noise" so that the $I_{noise}(t,T) = i_{noise}(t,T) I_c(T)$ satisfies following relations:

$$\left.\begin{array}{l} < I_{noise}(t,T) >_t = 0 \\ < I_{noise}(t,T) I_{noise}(t+t',T) >_t = \frac{2k_B T}{R_J} \delta(t') \end{array}\right\} \,, \quad (8)$$

where $< A(t) >_t$ means the time average of a time dependent function $A(t)$. The R_J is the resistance of a junction and is given as a function of $I_0 = i_0 I_c(T)$;

$$\frac{1}{R_J} = \frac{1}{R_{QP}^{(eff)}(I_0)} + \frac{1}{R_{shunt}} \equiv \frac{1}{R_J(I_0)} \,, \quad (9)$$

where R_{shunt} is a shunt resistance added externally per a junction, and $R_{QP}^{(eff)}(I_0)$ is an effective resistance of a junction due to QP tunneling.

The white noises are made numerically by using random numbers. We write here the random numbers as $i_{Random}^{(Cal)}(t)$, which have been made by the normal random number generator in the library program. The normalized white noise $i_{noise}(t,T)$ defined by $I_{noise}(t,T)/I_c(T)$ must be proportional to $i_{Random}^{(Cal)}(t)$, that is,

$$i_{noise}(t,T) = \eta(T) i_{Random}^{(Cal)}(t) \,. \quad (10)$$

The autocorrelation $< i_{noise}(t,T) i_{noise}(t+t',T) >_t$ is equal to $\eta(T)^2 < i_{Random}^{(Cal)}(t) i_{Random}^{(Cal)}(t+t') >_t$. Therefore, by using relation (8) and doing an integral over the t', we get

$$\frac{2k_B T}{I_c(T)^2 R_J} = \eta(T)^2 \int_{-\infty}^{\infty} < i_{Random}^{(Cal)}(t) i_{Random}^{(Cal)}(t+t') >_t dt' \,. \quad (11)$$

Here we define an absolute time resolution Δt. By doing some numerical calculations for the kernel defined by Eqs.(27) and (28), I found that the time resolution Δt with the value of 1×10^{-14}s(=10fs) is small enough to resolve the structure of the kernel. [35] The autocorrelation $<$

$i_{Random}^{(Cal)}(t) i_{Random}^{(Cal)}(t + t') >_t$ is also proportional to the delta function $\delta(t')$, so that the integral in Eq.(11) can be well evaluated as $< i_{Random}^{(Cal)}(t)^2 >_t \Delta t$. Therefore, the $\eta(T)$ is given by

$$\eta(T) = \sqrt{\frac{2k_B T}{< i_{Random}^{(Cal)}(t)^2 >_t \Delta t \, I_c(T)^2 R_J}} \, , \tag{12}$$

so that from Eq.(10) we can get the normalized white noise $i_{noise}(t, T)$ at a finite temperature T as full numerical data with a function of time t defined by $n\Delta t$. All the experiments always include the effect of thermal noise. Therefore, all the calculations presented in the present paper also include the effect of the thermal noise, except for the special case that I notice. In the present study, the sample temperature T has been set to 4.2K.

By using the dimensionless time τ defined by $\omega_r t/2\pi(= f_r t)$ and the normalized distance ν defined by x/λ_J, equation (2) can be rewritten as

$$\begin{pmatrix} Q_1(\nu, \tau) \\ \cdot \\ Q_\ell(\nu, \tau) \\ \cdot \\ Q_N(\nu, \tau) \end{pmatrix} = \left(2\pi \frac{f_p^*}{f_r} \right)^2 \mathbf{\Sigma_L}^{-1} \mathbf{\Sigma_c} \frac{\partial^2}{\partial \nu^2} \begin{pmatrix} \varphi_1(\nu, \tau) \\ \cdot \\ \varphi_\ell(\nu, \tau) \\ \cdot \\ \varphi_N(\nu, \tau) \end{pmatrix} \, , \tag{13}$$

where f_p^* is the effective plasma frequency of a junction calculated as $\sqrt{J_c d_c'/2\pi\Phi_0\varepsilon\varepsilon_0}$. In the MS-unified theory, the effect of the magnetic field is taken into account via the boundary condition at the junction edge. Therefore, we solve Eq.(13) under the boundary condition such that

$$\left. \frac{\partial \varphi_\ell(\nu, \tau)}{\partial \nu} \right|_{edge} = \frac{B_{eff}^{(\ell)}}{\mu_0 J_c \lambda_J} (1 + 2\Sigma_L) \, , \tag{14}$$

where $B_{eff}^{(\ell)}$ is an effective magnetic induction at the edge of the ℓ-th IJJ. By solving Eq.(13) full numerically, we can get the gauge-invariant phase differences $\varphi_\ell(\nu, \tau)$ of all the junctions $\ell = 1, 2, \cdots, N$ as a function of ν and τ. In the present paper, not only the case such as SIS-IJJs but also the case in which some insulating(I) layers in IJJs are replaced by ferromagnetic(F) layers is considered. The F-layer makes a magnetization M, therefore, if the ℓ-th I-layer is replaced by the F-layer with $M = M^{(\ell)}$, then the $B_{eff}^{(\ell)}$ in Eq.(14) is given in SI-units as

$$B_{eff}^{(\ell)} = B_{ext} + M^{(\ell)} \, . \tag{15}$$

For the SFS-junctions, there are many excellent works. [37–44] Especially, two review papers by Golubov et al. [39] and Buzdin [40] include many valuable information. Recently, the phase dynamics induced by spin waves in a SFS Josephson junction consisting of *s*-wave superconductors have been numerically studied within the framework of the resistively shunted junction (RSJ) model. [44] The calculations by Hikino et al. [44] have told us that the magnetization of F-layer plays an essential role to understand the nature of phase dynamics. In the SFS-junction, it is well known that the amplitude of the CP-tunneling critical current *oscillatory* varies as a function of the thickness d_F of the F-layer [40], which is called as "0-π

transition". The first crossover thickness $d_F^{(1)}$, in which the nature of junction changes from the 0 to the π state, is about 50Å for the SFS-junction using an NiCu-system ferromagnetic metal. [40, 43] As can be seen later, the barrier thickness d of BSCCO IJJs is 12Å. In the present paper, therefore, two cases are considered; one is the case in which the correction for the amplitude of the CP tunneling current is considered and other is not.

The $Q_\ell(\nu, \tau)$ in Eq.(13) is

$$Q_\ell(\nu,\tau) = \frac{\partial^2 \varphi_\ell(\nu,\tau)}{\partial \tau^2} + 2\pi \frac{f_p^*}{f_r} \frac{1}{\sqrt{\beta_c^*(i_0, J_c, SR_{shunt})}} \frac{\partial \varphi_\ell(\nu,\tau)}{\partial \tau}$$
$$+ \left(2\pi \frac{f_p^*}{f_r}\right)^2 \left\{ \sum_{\ell'=1}^{N} \{\boldsymbol{\Sigma_c}\}_{\ell,\ell'} \chi_{\ell'}(d_F) i_{CP}^{(\ell')}(\nu,\tau) - i_{ext}(\tau) \right\}. \qquad (16)$$

Here note that we generally consider the case including the F-layer, so that the correction term $\chi_\ell(d_F)$ which has not been written in Eq.(6) has been added into Eq.(16). The $\chi(d_F)$ is defined by $I_c^{(F)}(d_F)/I_c^{(NM)}$ using the critical currents $I_c^{(F)}(d_F)$ and $I_c^{(NM)}$ of the SFS and SIS Josephson junctions, and the value of $\chi_\ell(d_F)$ oscillatory varies as a function of d_F bewteen 0 to 1 when the ℓ-th junction includes F-layer. Here it is clear that $\chi_\ell(d_F) = 1$ when the ℓ-th junction includes no F-layer. For example, $\chi(d_F)$ can be written as [40]

$$\chi(y) = 4y \left| \frac{\cos 2y \sinh 2y + \sin 2y \cosh 2y}{\cosh 4y - \cos 4y} \right|, \qquad (17)$$

where $y \equiv d_F/\xi_F$ and ξ_F is the characteristic length of the superconducting correlation decay with oscillations in the F layer. [40] The $\chi(y)$ as a function of $2y$ is drawn in Fig.11 in the review paper by Buzdin. [40]

By using the McCumber parameter $\beta_c(i_0, J_c, SR_{shunt})$, [35] the $\beta_c^*(i_0, J_c, SR_{shunt})$ in Eq.(16) can be written as

$$\frac{1}{\sqrt{\beta_c^*(i_0, J_c, SR_{shunt})}} = \frac{\Phi_0 f_p^*}{J_c SR_{shunt}} + \frac{\Phi_0 f_p^*}{I_c R_{QP}^{(eff)}(I_0)}$$
$$= \gamma_p \left\{ \frac{\Phi_0 f_p}{J_c SR_{shunt}} + \mu(i_0) \right\}$$
$$= \frac{\gamma_p}{\sqrt{\beta_c(i_0, J_c, SR_{shunt})}}, \qquad (18)$$

where

$$\gamma_p \equiv \frac{f_p^*}{f_p} = \sqrt{\frac{d_c'}{d}}. \qquad (19)$$

It should be noted here that the $\mu(i_0)$ in Eq.(18) is a universal curve as a function of only the normalized external dc i_0 so that this curve is always valid for all the IJJs in BSCCO characterized by the $d_{x^2-y^2}$ symmetry superconducting gap. [35] Namely, if the no shunt case, i.e., the case of $R_{shunt} \rightarrow \infty$, is considered, then the McCumber parameter of BSCCO is given as a function of only the i_0 such as $\mu^{-2}(i_0)$. [35] Here I wish to say that when the effect of electric field coupling is not considered, the plasma frequencies ratio γ_p is equal to 1 and

the matrix Σ_c is equal to the unit matrix $\mathbf{1}$, therefore, the $Q_\ell(\nu, \tau)$ for this case is just equal to the left-hand side of Eq.(31) in my recent paper. [35] We will see later that $\gamma_p \simeq 1$ and $\Sigma_c \simeq \mathbf{1}$ even if the effect of the electric field coupling is considered for BSCCO IJJs.

Kautz and Monaco extensively studied the nature of Shapiro steps on the SIS Josephson junction [45]. As a result, they found that there is a chaotic region in which Shapiro steps cannot be observed. The chaotic region is found between f_{RC} and f_p, i.e., $f_{RC} \leq f_r \leq f_p$. In my previous paper, [35] I have already pointed out that the lower frequency f_{RC} of the chaotic region is given by

$$\left. \begin{array}{l} f_{RC} = f_{RC}^{(NS)}(i_0) + f_{RC}^{(Shunt)}(SR_{shunt}) \\ f_{RC}^{(Shunt)}(SR_{shunt}) = \frac{1}{2\pi R_{shunt}C} \end{array} \right\} . \tag{20}$$

Moreover, I have mentioned that the frequency $f_{RC}^{(NS)}(i_0)$ for the case of no-shunt (NS) resistance is given by using a universal curve $\mu(i_0)$ as

$$f_{RC}^{(NS)}(i_0) = f_p \mu(i_0) . \tag{21}$$

Above two equations (20) and (21) tell us that the SR_{shunt}-product is an important parameter to understand the nature of Shapiro step observed on the BSCCO IJJ.

If the case such that $B_{ext} = 0$ and there are no F-layers in IJJs is considered, then the $\partial \varphi_\ell(\nu, \tau)/\partial \nu$ is zero for all junctions. Therefore, the equation (13) for the present case is equivalent to the equation $Q_\ell(\nu, \tau) = 0$. Equation (16) tells us that the equation $Q_\ell(\nu, \tau) = 0$ reflects *only* the electric interaction between neighboring Josephson junctions. It is clear that if $\Sigma_c = \mathbf{1}$ and $\chi_\ell(d_F) = 1$ for all ℓ, then the equation $Q_\ell(\nu, \tau) = 0$ is just equal to equation(31) in my recent paper. [35] In order to see the effects originated from both the electric and magnetic interactions, we must solve Eq.(13) with a finite value of B_{ext}, so that the Eq.(13) becomes a matrix form including not only Σ_c but also Σ_L describing the magnetic interaction between neighboring Josephson junctions.

The dc voltage $< V_\ell >$ observed on the ℓ-th IJJ satisfies

$$\varepsilon \varepsilon_0 \frac{L_x L_y}{d} < V_\ell > = \int dQ = \int_0^{L_x} \varepsilon \varepsilon_0 \frac{L_y}{d} < V_\ell(x,t) >_t dx , \tag{22}$$

where L_x and L_y are junction lengths along the x and y axes, i.e., $S = L_x L_y$, and $< V_\ell(x,t) >_t$ means the time average of $V_\ell(x,t)$ which is a voltage of the ℓ-th IJJ as a function of x and t. Therefore, the dc voltage $< V_\ell >$ for the ℓ-th IJJ is simply given by

$$< V_\ell > = \frac{1}{L_x} \int_0^{L_x} < V_\ell(x,t) >_t dx , \tag{23}$$

so that the total dc voltage $< V >_{total}$ observed experimentally is given by

$$< V >_{total} = \sum_{\ell=1}^{N} < V_\ell > \equiv N < V >_{reduce} , \tag{24}$$

where $< V >_{reduce}$ is the reduced voltage when $< V >_{total}$ is assumed as a simple sum of N-junctions system. The $< V_\ell(x,t) >_t$ is the same as Eq.(33) in my previous paper [35], that

is,

$$< V_\ell(x,t) >_t = \frac{\Phi_0 f_r}{2\pi} \frac{\varphi_\ell(x,\tau_2) - \varphi_\ell(x,\tau_1)}{\tau_2 - \tau_1} \ . \tag{25}$$

Here, we must remember that τ_1 and τ_2 must be intergers in order to get a very well converged value for an averaging between τ_1 and τ_2. [35]

The general form of $i_{CP}^{(\ell)}(\nu,\tau)$ is given by [35]

$$i_{CP}^{(\ell)}(\nu,\tau) = \int_{-\infty}^{\tau} K_{CP}^{(\ell)}(\tau-\tau') \sin \frac{\varphi_\ell(\nu,\tau') + \varphi_\ell(\nu,\tau)}{2} d\tau' \ , \tag{26}$$

where the kernel $K_{CP}^{(\ell)}(\tau-\tau')$ can be written as

$$K_{CP}^{(\ell)}(\tau-\tau') = \frac{2\pi}{\hbar\omega_r} \kappa_{CP}^{(\ell)}(\tau-\tau') \ , \tag{27}$$

$$\kappa_{CP}^{(\ell)}(\tau-\tau') =$$

$$\frac{\sum_{\mathbf{k}}^{BZ_1} \sum_{\mathbf{k}'}^{BZ_1} \left|H_{\mathbf{k},\mathbf{k}'}'^{(\ell)}\right|^2 \frac{|\Delta_{\mathbf{k}}\Delta_{\mathbf{k}'}|}{E_{\mathbf{k}}E_{\mathbf{k}'}} \left[\begin{array}{l} \{f(E_{\mathbf{k}}) - f(E_{\mathbf{k}'})\} \sin\left\{ \frac{E_{\mathbf{k}} - E_{\mathbf{k}'}}{\hbar\omega_r} 2\pi(\tau-\tau') \right\} \\ + \{1 - f(E_{\mathbf{k}}) - f(E_{\mathbf{k}'})\} \sin\left\{ \frac{E_{\mathbf{k}} + E_{\mathbf{k}'}}{\hbar\omega_r} 2\pi(\tau-\tau') \right\} \end{array} \right]}{\sum_{\mathbf{k}}^{BZ_1} \sum_{\mathbf{k}'}^{BZ_1} \left|H_{\mathbf{k},\mathbf{k}'}'^{(\ell)}\right|^2 \frac{|\Delta_{\mathbf{k}}\Delta_{\mathbf{k}'}|}{E_{\mathbf{k}}E_{\mathbf{k}'}} \left[\frac{f(E_{\mathbf{k}}) - f(E_{\mathbf{k}'})}{E_{\mathbf{k}} - E_{\mathbf{k}'}} + \frac{1 - f(E_{\mathbf{k}}) - f(E_{\mathbf{k}'})}{E_{\mathbf{k}} + E_{\mathbf{k}'}} \right]} \ , \tag{28}$$

where BZ_1 means the 1st Brillouin zone, $f(E)$ is the Fermi-Dirac distribution function and $H_{\mathbf{k},\mathbf{k}'}'^{(\ell)}$ is the matrix element due to the $\mathbf{k} \to \mathbf{k}'$ tunneling in the ℓ-th IJJ. Here it should be noted that the $H_{\mathbf{k},\mathbf{k}'}'^{(\ell)}$ for the coherent tunneling is proportional to $\delta_{\mathbf{k},\mathbf{k}'}$ and that for the incoherent one is given by a constant irrespective of $\mathbf{k}$ and $\mathbf{k}'$. In the practical calculations of $\kappa_{CP}^{(\ell)}(\tau - \tau')$ defined by Eq.(28), therefore, $H_{\mathbf{k},\mathbf{k}'}'^{(\ell)}$ is set to $\delta_{\mathbf{k},\mathbf{k}'}$ for the coherent tunneling and to 1 for the incoherent one. The quasiparticle excitation energy $E_{\mathbf{k}}$ is given by $\sqrt{\xi_{\mathbf{k}}^2 + \Delta_{\mathbf{k}}^2}$. The $\Delta_{\mathbf{k}}$ is the superconducting energy gap and it is well known that the $\Delta_{\mathbf{k}}$ of d-wave symmetry superconductor is represented as $\Delta(T)\cos 2\phi_k$, where ϕ_k is the angle of $\mathbf{k}$-vector measured from x-axis. [10] The $\xi_{\mathbf{k}}$ is the one-electron energy relative to the Fermi level. By doing the band structure calculation, I got the values of $\xi_{\mathbf{k}}$ as full numerical data. [46]

In my previous paper, [35] I have carried out the sophisticated numerical calculations in which two types of CP tunneling currents such as coherent and incoherent ones have been correctly calculated within the framework of the $d_{x^2-y^2}$ symmetry superconducting gap, and found that the resultant I-V characteristics very well coincide with the result calculated in a usual way such as $i_{CP}(\tau) = \sin\varphi(\tau)$. [35] This finding is come from the fact that Shapiro steps are observed on the quasiparticle (QP) branch of the I-V characteristics so that the Shapiro steps are not so sensitive to the CP tunneling *mechanism*. [35] In the present paper, therefore, we evaluate $i_{CP}^{(\ell)}(\nu,\tau)$ as $\sin\varphi_\ell(\nu,\tau)$, in order to save the CPU times on the numerical calculations.

3. Calculation

We consider here the BSCCO high-T_c superconductors. The typical values of electrode thickness w, barrier thickness d and London penetration depth λ_L are 3, 12 and 1700Å,

the 1@5 and 5@5 junctions, which are surface junctions, show the same characteristics and the 2@5 and 4@5 ones (intermediate junctions) also show the same nature.

In the following, previous results calculated for no F-layers, i.e., $M^{(\ell)} = 0$ for all the IJJs, are first presented, and next the results for $M^{(\ell)} \neq 0$ are given. Here note that in the present calculations, *an ℓ-th insulating (I) layer in BSCCO IJJs is replaced by a F-layer which makes a magnetization with the value of $M^{(\ell)}$.*

4. Results and discussion

4.1 Effect of L_x

It is important to check the effect of junction length L_x along the x-axis into the I-V characteristics. In my previous paper, [36] I have calculated the I-V characteristics for three shapes $(L_x, L_y) = (2.5, 10)$, $(5, 5)$ and $(10, 2.5)$ in μm with the same junction cross section $S(= L_x L_y) = 25\mu$m^2. The calculated results have told us that the overall profiles of the I-V characteristics calculated for the same external magnetic induction are fairly similar each other. This finding is reasonable since all the junction lengths L_x considered here satisfy the condition of $L_x > \lambda_J (= 0.3687\mu$m$)$, that is, all the junctions adopted in the calculations belong to the category of so-called "large junction". In the following, therefore, only the square junction ($L_x = L_y = 5\mu$m) is considered for simplicity.

4.2 Effect of SR_{shunt}-product

The SR_{shunt}-product is an important parameter to understand the nature of Shapiro step. In my previous papers, [35, 36] I *extensively* studied the effect of the SR_{shunt}-product to the I-V characteristics. In the present paper, therefore, only the conclusions obtained are briefly presented.

First, from the calculations for a single junction, I have found that (I) the value of shunt resistance R_{shunt} added externally should be small such as 1Ω/junction, i.e., SR_{shunt}/junction= 25μm$^2\Omega$, if we wish to make a Shapiro step device which is *hard* for the external magnetic disturbance, and (II) in the case of the large R_{shunt}-value such as 5Ω/junction, not only the 1st-order Shapiro steps but also the Fiske steps [47, 48] are found, especially, in the case of the low magnetic field. Next, from the calculations for multi junctions such that $N = 5, 6$ and R_{shunt}/junction= 1, 2, 3, 4 and 5Ω, I have found that (III) the 1st-order Shapiro steps are found when R_{shunt}/junction$\leq$ 3Ω, but no detectable Shapiro steps are found when R_{shunt}/junction= 4 and 5Ω, and (IV) this result directly reflects the nature of the magnetic interactions between the neighboring Josephson junctions.

From the above results, I have concluded that it is essential to add the shunt resistance with a low-value into the BSCCO IJJs, if we wish to make a good quality Shapiro step device. In the present study, therefore, the value of SR_{shunt}/junction is fixed to 50μm$^2\Omega$.

4.3 Effect of i_r

We consider here the effect of the normalized amplitude i_r of the external ac modulation current $i_r \sin \omega_r t$. In order to do so, first, I have calculated the I-V characteristics with no external magnetic field, i.e., $\alpha = 0$, under the condition such that $J_c = 1000$A/cm^2,

$f_p = 122$GHz, $f_r = 200$GHz, $SR_{shunt}/$junction$= 50\mu$m$^2\Omega$ and $N = 5$. Those are drawn as (i), (ii) and (iii) in Fig.1 for $i_r = 0$, 1 and 2 which are denoted as $(i_r, \alpha) = (0, 0)$, $(1, 0)$ and $(2, 0)$, respectively. Next, I have calculated the I-V characteristics with finite external magnetic fields, i.e., $\alpha \neq 0$, under the same condition as in Fig.1. Here note again that the external magnetic induction B_{ext} is defined by $\alpha B_0(L_x)$ and the $B_0(L_x)$ is 0.345T for $L_x = 5\mu$m. The I-V characteristics calculated for $(i_r, \alpha) = (0, 0.5)$, $(0, 1)$, $(0, 2)$, $(1, 0.5)$, $(1, 1)$, $(1, 2)$, $(2, 0.5)$, $(2, 1)$ and $(2, 2)$ are shown in Fig.2(a), (b), (c), (d), (e), (f), (g), (h) and (i), respectively.
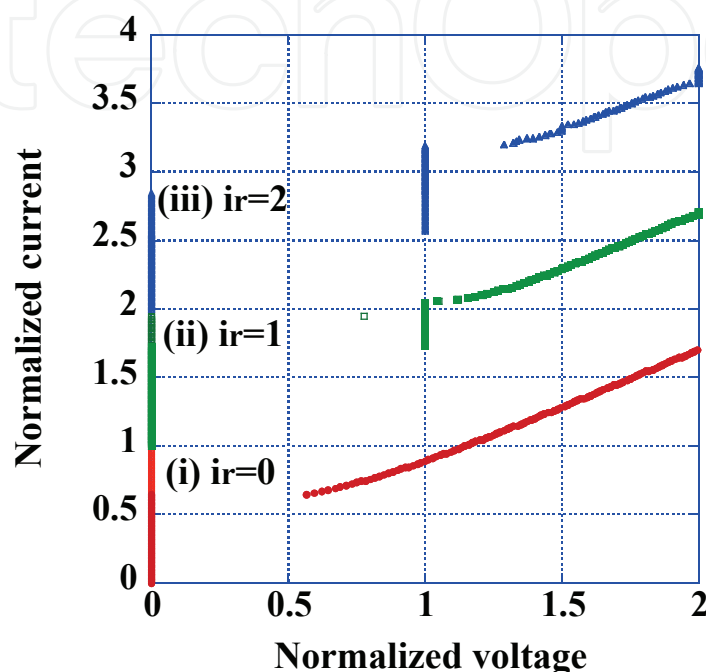

Fig. 1. The I-V characteristics with no external magnetic field, i.e., $\alpha = 0$, calculated for $N = 5$, $J_c = 1000$A/cm^2, $f_p = 122$GHz, $f_r = 200$GHz, $L_x = 5\mu$m, $S(= L_x L_y) = 25\mu$m^2, and $SR_{shunt}/$junction$= 50\mu$m$^2\Omega$. The effect of charge coupling is not taken into account. (i), (ii) and (iii) are those for $i_r = 0$, 1 and 2, and are denoted as $(i_r, \alpha) = (0, 0)$, $(1, 0)$ and $(2, 0)$, respectively. Note that the I-V characteristics (ii) and (iii) have been shifted by 1 and 2 along the vertical axis, and that the (ii) is basically the same as the I-V characteristics (b) in Fig.10 in my previous paper. [35] It is also noted that no external magnetic field is applied, so that all the SIS-junctions show exactly the same characteristics because the no charge coupling case is considered. Namely, a relation "1@N = 2@N = $\cdots$ = N@N" is satisfied for the I-V characteristics of respective junctions. The horizontal axis indicates the dc voltage normalized to $\Phi_0 f_r$, and the vertical one shows the normalized dc i_0. Shapiro steps are clearly found when the external ac modulation current is applied, i.e., $i_r \neq 0$.

First, let us focus our attention to the results calculated for $i_r = 0$, i.e., $(i_r, \alpha) = (0, 0)$ in (i) in Fig.1 and $(0, 0.5)$, $(0, 1)$ and $(0, 2)$ in Fig.2(a), (b) and (c), respectively. Since $i_r = 0$, these results directly show the change of the I-V characteristics due to the change of the external magnetic field. We can see that (I) the critical current decreases with the increasing the external magnetic induction B_{ext}, (II) this trend is remarkable in inner junctions 2@5, 3@5 and 4@5 rather than surface junctions 1@5 and 5@5, and (III) the central junction 3@5 shows a large change due to the change of the B_{ext}. Flux quanta enter the insulating layers when $B_{ext} \neq 0$. If we consider the case when a flux quantum just enters an insulating layer in the stacked junctions consisting
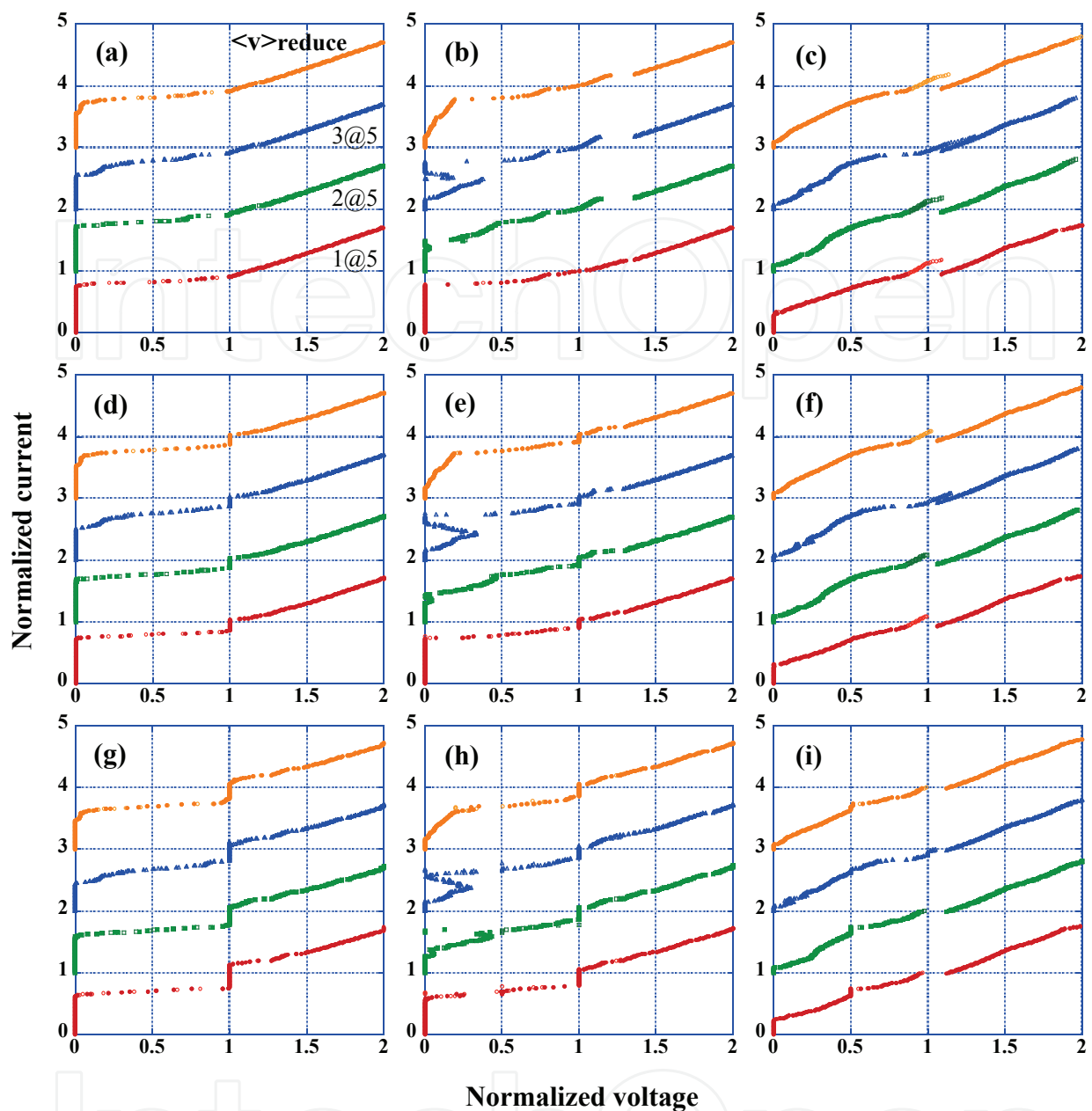
Fig. 2. The *I-V* characteristics of BSCCO IJJs calculated for the same condition as in Fig.1, except for the external magnetic induction B_{ext}. The B_{ext} is defined by $\alpha B_0(L_x)$ and the $B_0(L_x)$ is 0.345T because of $L_x = 5\mu$m. The (i_r, α) of (a), (b), (c), (d), (e), (f), (g), (h) and (i) are $(0, 0.5)$, $(0, 1)$, $(0, 2)$, $(1, 0.5)$, $(1, 1)$, $(1, 2)$, $(2, 0.5)$, $(2, 1)$ and $(2, 2)$, respectively. The reduced voltage $< V >_{reduce}$ defined by Eq.(24) is also shown. Shapiro steps are found when $i_r \neq 0$, but not so clear when $\alpha = 2$.

of the odd number of junctions, then it is sure that *its* flux quantum must enter the insulating layer of central SIS Josephson junction such as 3@5 junction because of the symmetry of the odd number of junctions. This is reasonable to the finding (III). Actually, in the case of Fig.2(a), we can see that only the 3@5 central junction just shows the voltage due to the flux flow when i_0 is about 0.6.

As can be seen in Fig.1, the height of Shapiro steps increases with the increasing the i_r. By comparing the calculated results for $i_r \neq 0$ shown in Fig.2(d), (e), (f), (g), (h) and (i) with those for $i_r = 0$ shown in Fig.2(a), (b) and (c), we can say that the *I-V* characteristics calculated for $(i_r, \alpha) = (1, 0.5), (1, 1), (1, 2), (2, 0.5), (2, 1)$ and $(2, 2)$ could be regarded as those for $(i_r, \alpha) = (0, 0.5), (0, 1)$ and $(0, 2)$ *added* Shapiro steps which have been calculated by taking into account the effect of the external magnetic field. The *I-V* characteristics for $i_r = 0$ shown in Fig.2(a), (b) and (c) *directly* reflect the nature of flux flow, and the Shapiro steps shown in Fig.2(d), (e), (f), (g), (h) and (i) are originated from the coupling between the ac Josephson effect and the external ac modulation current with $i_r \neq 0$. Therefore, the calculated results shown in Fig.2 seem to show that the Shapiro step and flux flow could be treated separately under the presence of the external magnetic field.

4.4 Effect of B_{ext}

We shall consider here the effect of the external magnetic field B_{ext} on the reduced voltage $< V >_{reduce}$ defined by Eq.(24) which is directly connected with the experimental *I-V* characteristics. By setting the calculation condition to such that $J_c = 1000 A/cm^2$, $f_p = 122 GHz$, $f_r = 200 GHz$, R_{shunt}/junction= 2Ω, SR_{shunt}/junction= $50\mu m^2\Omega$, $i_r = 1$ and $L_x = 5\mu m$, i.e., $B_0(L_x) = 0.345T$, I have calculated the *I-V* characteristics as a function of α, which defines the external magnetic induction B_{ext} as $\alpha B_0(L_x)$, and the number N of stacked junctions. The values from 0 to 2 with 0.1-step have been selected as the α and two values 1 and 5 have been adopted as the N. The normalized height $\Delta i_1(\alpha, N)$ of the 1st-order Shapiro step and the normalized critical current $i_c(\alpha, N)$ evaluated from the reduced voltage $< V >_{reduce}$ are plotted in Fig.3 as a function of α.

Figure 3 shows that (I) for almost all the α-values, the values of $\Delta i_1(\alpha, 1)$ drawn by open circles are somewhat larger than those of $\Delta i_1(\alpha, 5)$ by solid circles, but its difference is not so large, i.e., the α-dependence of $\Delta i_1(\alpha, N)$ seems to be very similar even if the value of N differs each other such as $N = 1$ and 5. For the $i_c(\alpha, N)$, we can see that (II) the α-dependence of the $i_c(\alpha, 1)$ drawn by open squares largely differs from that of the $i_c(\alpha, 5)$ by solid squares. In the BSCCO IJJs with a stacking structure, there are considerable magnetic interactions between neighboring Josephson junctions when $\alpha \neq 0$. Therefore, the finding (II) clearly tells us that (III) the normalized critical current is strongly affected by the magnetic interaction between neighboring Josephson junctions.

4.5 Effect of ferromagnetic layer

As the case in which some insulating(I) layers in BSCCO-IJJs are replaced by ferromagnetic(F) ones, there are many cases. In this section, for the simplicity we consider the case such that only the ℓ-th I-layer in the BSCCO-IJJs is replaced by a F-layer whose value of the magnetization is $M(B_{ext})$ as a function of the external magnetic field B_{ext}. The magnetization curve $M(B_{ext})$ is characterized by three points; one is the saturation magnetization $M_{sat}(\neq 0)$ in which $dM/dB_{ext} = 0$, two is the residual magnetization $M_{res}(\neq 0)$ in which $B_{ext} = 0$, and three is the coercive force in which the magnetization is zero for the non-zero external field, i.e., $M(B_{ext} = B_{coe} \neq 0) = 0$. We consider here the non-zero magnetization case so that the case of coercive force is not considered here. The M_{sat} is obtained when a magnetic field B_L which is large enough to satisfy the condition of $dM/dB_{ext} = 0$ is applied to the F-layer, i.e.,
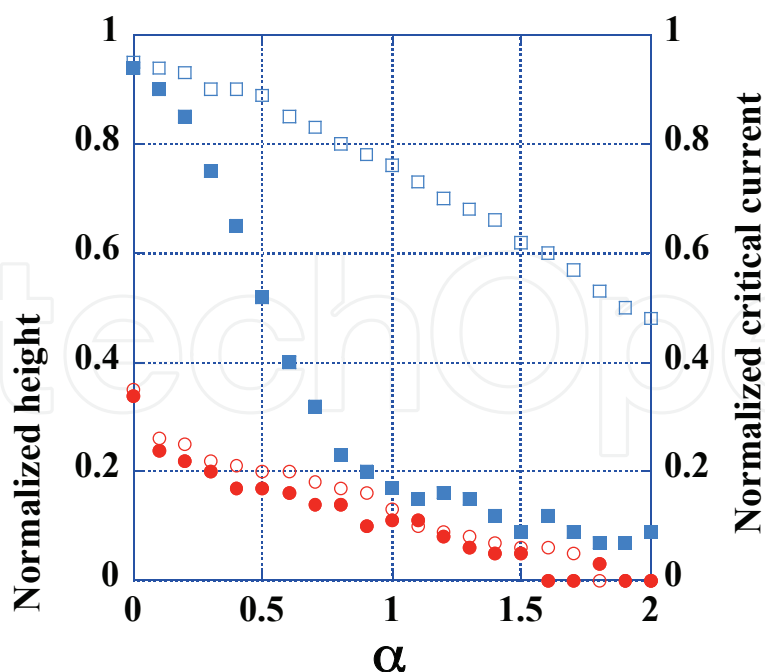
Fig. 3. Normalized height $\Delta i_1(\alpha, N)$ of the 1st-order Shapiro step and the normalized critical current $i_c(\alpha, N)$ as a function of α and N. In this figure, the values of α have been selected from 0 to 2 with 0.1-step, and two values 1 and 5 have been adopted as the number N of junctions. The calculation condition is that $J_c = 1000\text{A}/\text{cm}^2$, $f_p = 122\text{GHz}$, $f_r = 200\text{GHz}$, $L_x = 5\mu\text{m}$, R_{shunt}/junction$= 2\Omega$, and $i_r = 1$. As already stated, the external magnetic induction B_{ext} is defined by $\alpha B_0(L_x)$ and the $B_0(L_x)$ is 0.345T because of $L_x = 5\mu\text{m}$. The $\Delta i_1(\alpha, 1)$ and $\Delta i_1(\alpha, 5)$ are indicated by open and solid circles, respectively, and the $i_c(\alpha, 1)$ and $i_c(\alpha, 5)$ are drawn by open and solid squares, respectively. In the present paper, the effect of thermal noise has been always taken into account in all the calculations, so it must be stated that both the values of $i_c(0, 1)$ and $i_c(0, 5)$ are somewhat smaller than 1. The effect of charge coupling is not taken into account.

$M_{sat} = M(B_{ext} \geq B_L)$, but the strength of the B_L strongly depends on the magnetic property of the F-layer. On the contrary to the case of M_{sat}, the M_{res} is obtained when $B_{ext} = 0$, i.e., $M_{res} = M(0)$, so it is expected that it could be much easier to control the sample condition as compared with the case of M_{sat}.

The sizable effect for the magnetic field is mainly found in the 3@5 central junction as can be seen from Fig.2 for $N = 5$. In the following, therefore, first we focus our attention to the case such that the I-layer in the 3@5 central SIS-Josephson junction is replaced by the F-layer, hereafter we call it as "central case", and next the cases for 1@5 and 2@5 junctions are considered, called as "surface and intermediate cases". Equation (15) tells us that the effective magnetic induction $B_{eff}^{(j)}$ at the edge of the j-th IJJ is given by

$$B_{eff}^{(j)} = B_{ext} + M(B_{ext})\delta_{j,\ell} . \tag{29}$$

The external magnetic induction B_{ext} is written as $\alpha B_0(L_x)$ using a constant magnetic induction $B_0(L_x)$ so that we write the magnetization $M(B_{ext})$ as $m(\alpha)B_0(L_x)$ using a dimensionless parameter $m(\alpha)$ as a function of α. The ℓ in Eq.(29) is 3, 1 and 2 for the

central, surface and intermediate cases, respectively. Therefore, the configuration $\mathbf{\Gamma}$ for the dimensionless effective magnetic induction defined by $B_{eff}^{(j)}/B_0(L_x)$ can be written as $(\alpha, \alpha, \alpha + m(\alpha), \alpha, \alpha)$, $(\alpha + m(\alpha), \alpha, \alpha, \alpha, \alpha)$ and $(\alpha, \alpha + m(\alpha), \alpha, \alpha, \alpha)$ for the central, surface and intermediate cases, respectively.

4.5.1 Case of $\chi_\ell(d_F) = 1$ for the ℓ-th SFS junction

First, we consider the case of the residual magnetization M_{res}, i.e., $\alpha = 0$. The configurations $\mathbf{\Gamma}$ for the central, surface and intermediate cases are therefore $(0, 0, m(0), 0, 0)$, $(m(0), 0, 0, 0, 0)$ and $(0, m(0), 0, 0, 0)$, respectively. By adopting the condition such that $N = 5$, $J_c = 1000 \text{A}/\text{cm}^2$, $f_p = 122\text{GHz}$, $f_r = 200\text{GHz}$, $R_{shunt}/\text{junction} = 2\Omega$, $SR_{shunt}/\text{junction} = 50\mu\text{m}^2\Omega$, $i_r = 1$ and $L_x = 5\mu\text{m}$, i.e., $B_0(L_x) = 0.345\text{T}$, I have calculated the I-V characteristics for $m(0) \equiv m_{res} = 0.1, 0.2, 0.5, 1$ and 2. The I-V characteristics of the central case calculated for $m_{res} = 0, 0.1, 0.2, 0.5, 1$ and 2 are shown in Fig.4(a), (b), (c), (d), (e) and (f), respectively. Here note that only the I-V characteristics of 1@5 surface, 2@5 intermediate and 3@5 central junctions are shown from a symmetry consideration. Figure 4 shows that (I) Shapiro steps are clearly found except for the 3@5 central junction when $m_{res} = 2$, and due to the increasing the m_{res}, i.e., the residual magnetization $M_{res} (\equiv m_{res} B_0(L_x))$, (II) the I-V characteristics of 3@5 central junction are gradually changed, but (III) those of other junctions including no F-layer almost remain the same, that is, no remarkable change is found for the junctions without the F-layer. These findings are interesting. We are now solving a matrix equation (13) with $\mathbf{\Sigma_c} = \mathbf{1}$. The matrix $\mathbf{\Sigma_L}$ describing the magnetic interactions between neighboring junctions is given by Eq.(3) so that the inverse matrix $\mathbf{\Sigma_L}^{-1}$ is not a diagonal but a general form in which all the matrix elements are not equal to zero. Therefore, except for the case of $\mathbf{\Gamma} = (0, 0, 0, 0, 0)$, it seems to be reasonable to suppose that the effect of ferromagnetic layer should be observed on not only the 3@5 central junction but also the others. The calculated results are far from such a conjecture. The results calculated for the surface and intermediate cases, namely, $\mathbf{\Gamma} = (m_{res}, 0, 0, 0, 0)$ and $(0, m_{res}, 0, 0, 0)$, are shown in Figs.5 and 6, respectively. From these figures, we can see a similar result as in Fig.4 such that (I) Shapiro steps are clearly found except for the junction including F-layer when $m_{res} = 2$, (II) the I-V characteristics of the junction including F-layer are gradually changed due to the increasing the m_{res}, but (III) no remarkable change is found for others.

From the above, we can conclude that if the case such that an I-layer in the BSCCO-IJJs is replaced by a F-layer is considered, then the effect of the F-layer to the I-V characteristics is restricted when $B_{ext} = 0$, namely, no remarkable change is found for the junctions without the F-layer.

Finally, let us consider the case of $B_{ext} \neq 0$, i.e., $\alpha \neq 0$. The configurations $\mathbf{\Gamma}$ to be considered are $(\alpha, \alpha, \alpha + m(\alpha), \alpha, \alpha)$, $(\alpha + m(\alpha), \alpha, \alpha, \alpha, \alpha)$ and $(\alpha, \alpha + m(\alpha), \alpha, \alpha, \alpha)$ for the central, surface and intermediate cases. As an example, in the following the α is set to 1 tentatively, and 0.1, 0.2, 0.5 and 1 are selected as the value of $m(1)$.

The I-V characteristics calculated for the central cases $(1, 1, 1 + m(1), 1, 1)$ with $m(1) = 0$, 0.1, 0.2, 0.5 and 1 are shown in Fig.7(a), (b), (c), (d) and (e), respectively, together with those for $\mathbf{\Gamma} = (2, 2, 2, 2, 2)$ shown in (f). Figure 7 shows that (I) Shapiro steps are clearly found
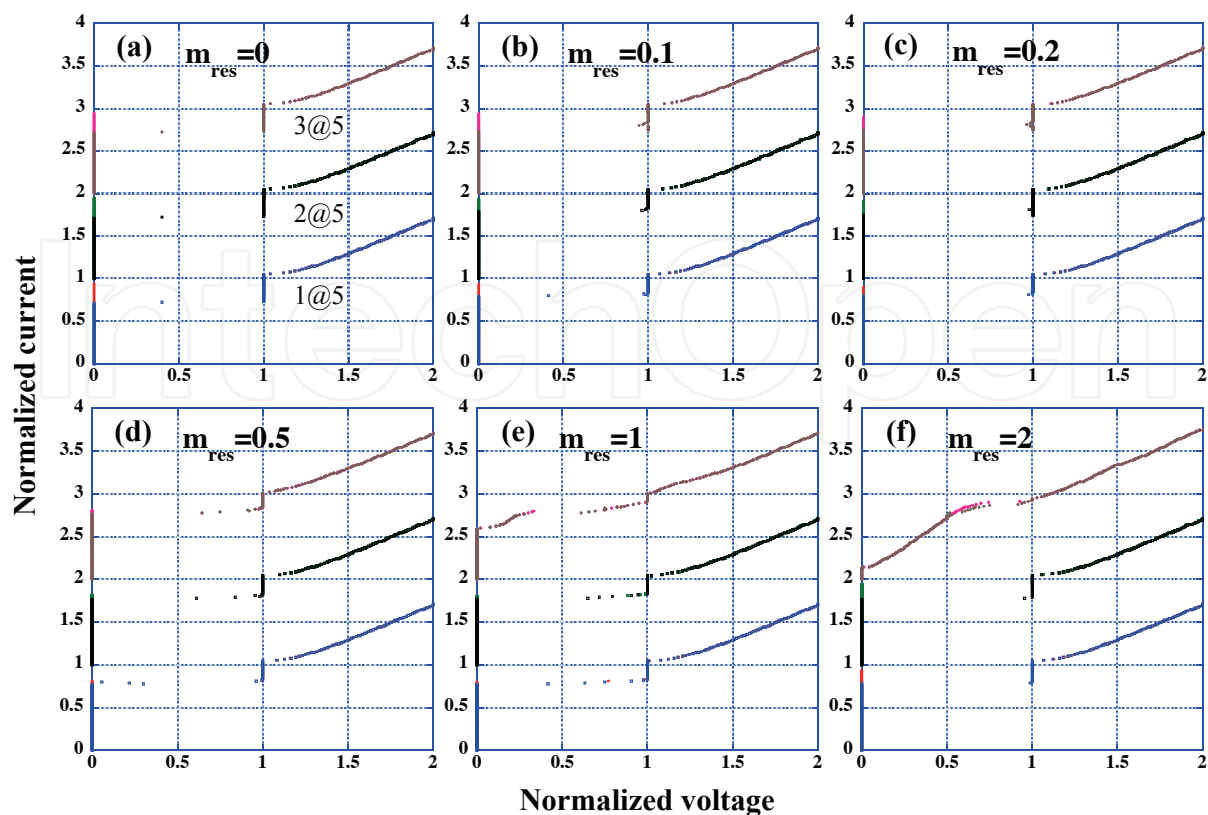
Fig. 4. The I-V characteristics of BSCCO IJJs calculated for $N = 5$, $J_c = 1000A/cm^2$, $f_p = 122GHz$, $f_r = 200GHz$, R_{shunt}/junction$= 2\Omega$, SR_{shunt}/junction$= 50\mu m^2\Omega$, $i_r = 1$, $L_x = 5\mu m$, i.e., $B_0(L_x) = 0.345T$ and $\chi_\ell(d_F) = 1$ for all junctions. The case such that there is no external magnetic field, i.e., $B_{ext} = 0$, and the I-layer in the 3@5 central SIS-Josephson junction is replaced by a F-layer is considered, so that the configuration Γ for the dimensionless effective magnetic induction defined by $B_{eff}^{(j)}/B_0(L_x)$ is $(0, 0, m_{res}, 0, 0)$. (a), (b), (c), (d), (e) and (f) are for $m_{res} = 0$, 0.1, 0.2, 0.5, 1 and 2, respectively. From the symmetry, only the I-V characteristics of 1@5 surface, 2@5 intermediate and 3@5 central junctions are shown. The horizontal axis indicates the dc voltage normalized to $\Phi_0 f_r$, and the vertical one shows the normalized dc i_0. Shapiro steps are clearly found except for the 3@5 central junction when $m_{res} = 2$ shown in (f).

in not only the junctions without F-layer but also the junction including F-layer, (II) the I-V characteristics of the 3@5 central junction including F-layer are surely changed due to the increasing the value of $m(1)$, but (III) those of other junctions without F-layer almost remain the same for the change of $m(1)$. Findings (II) and (III) mentioned now are fairly similar to those for the case of no external magnetic field, however, we wish to say that Shapiro step is found even in the 3@5 junction shown in (e) whose the Γ is $(1, 1, 2, 1, 1)$, in spite of the fact that clear Shapiro step cannot be found in (f) whose the Γ is $(2, 2, 2, 2, 2)$.

The I-V characteristics calculated for the surface case $(1 + m(1), 1, 1, 1, 1)$ are shown in Fig.8 and those for the intermediate one $(1, 1 + m(1), 1, 1, 1)$ are in Fig.9, where (a), (b) and (c) are for $m(1) = 0.2$, 0.5 and 1, respectively. Figure 8 shows that (I) Shapiro steps are clearly found in all the junctions even in the case of $m(1) = 1$, and (II) the I-V characteristics of 1@5 surface
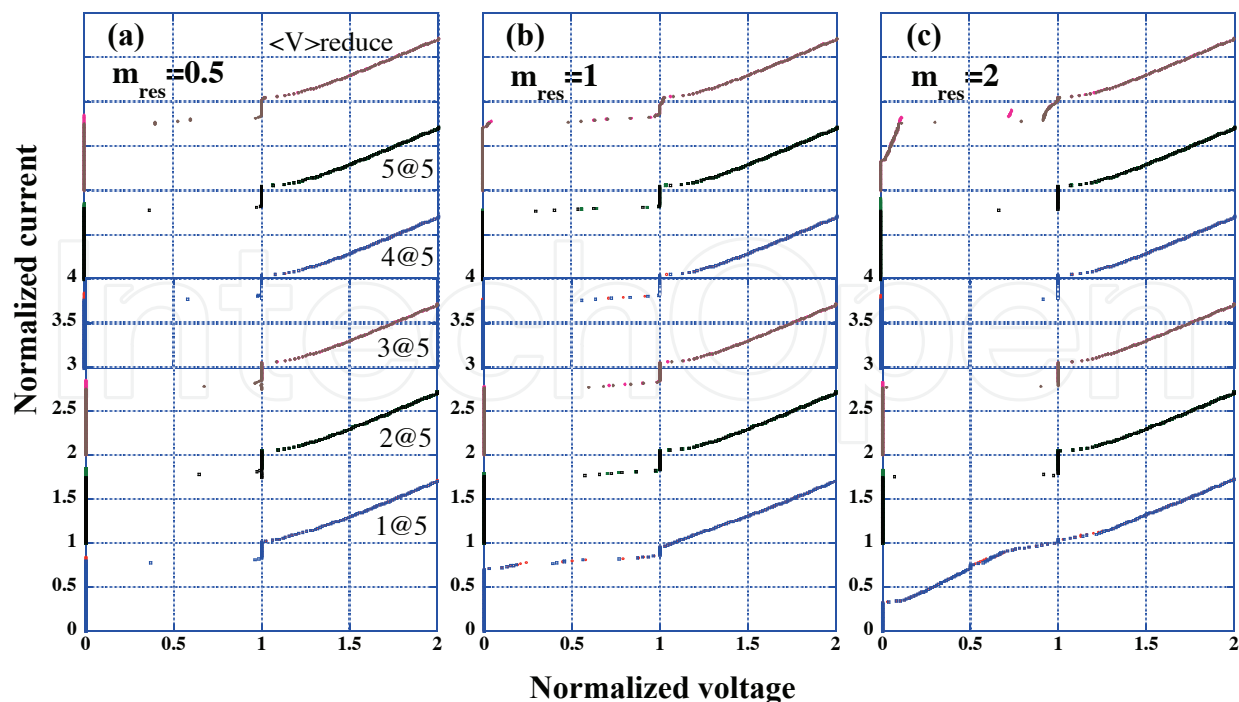
Fig. 5. The *I-V* characteristics of BSCCO IJJs calculated for $N = 5$, $J_c = 1000\text{A}/\text{cm}^2$, $f_p = 122\text{GHz}$, $f_r = 200\text{GHz}$, $R_{shunt}/\text{junction}= 2\Omega$, $SR_{shunt}/\text{junction}= 50\mu\text{m}^2\Omega$, $i_r = 1$, $L_x = 5\mu\text{m}$, i.e., $B_0(L_x) = 0.345\text{T}$, $B_{ext} = 0$ and $\chi_\ell(d_F) = 1$ for all junctions. The I-layer in 1@5 surface SIS junction is replaced by a F-layer so that the corresponding configuration **Γ** is $(m_{res}, 0, 0, 0, 0)$. Therefore, the *I-V* characteristics of all junctions are shown together with the reduced voltage $< V >_{reduce}$. (a), (b) and (c) are for $m_{res} = 0.5$, 1 and 2, respectively. The horizontal axis indicates the dc voltage normalized to $\Phi_0 f_r$, and the vertical one shows the normalized dc i_0. Shapiro steps are clearly found except for the 1@5 surface junction when $m_{res} = 2$ shown in (c).

junction including F-layer are gradually changed due to the increasing the value of $m(1)$. These findings are basically the same as the finding obtained in the central case. For the 2@5, 3@5, 4@5 and 5@5 junctions without F-layer, we can see that (III) the *I-V* characteristics of 2@5 and 3@5 junctions, which are close to the 1@5 junction including the F-layer, are fairly changed due to the increasing the $m(1)$, but (IV) those of 4@5 and 5@5 junctions, which are far from the 1@5 junction, almost remain the same as well as the central case. Finding (III) clearly tells us that the magnetic interaction between neighboring junctions is not negligible in BSCCO IJJs when $B_{ext} \neq 0$. From Fig.9, we can see a similar result as in the surface case, excepting 1@5 and 5@5 surface junctions in which the *I-V* characteristics are almost the same for the change of the value of $m(1)$.

4.5.2 Case of $\chi_\ell(d_F) < 1$ for the ℓ-th SFS junction

First, we consider the case of no external magnetic field, i.e., $\alpha = 0$. The calculation condition is the same as above, that is, $N = 5$, $J_c = 1000\text{A}/\text{cm}^2$, $f_p = 122\text{GHz}$, $f_r = 200\text{GHz}$, $R_{shunt}/\text{junction}= 2\Omega$, $SR_{shunt}/\text{junction}= 50\mu\text{m}^2\Omega$, $i_r = 1$ and $L_x = 5\mu\text{m}$, i.e., $B_0(L_x) = 0.345\text{T}$. There are three cases as the configurations that we should study, but in the following,
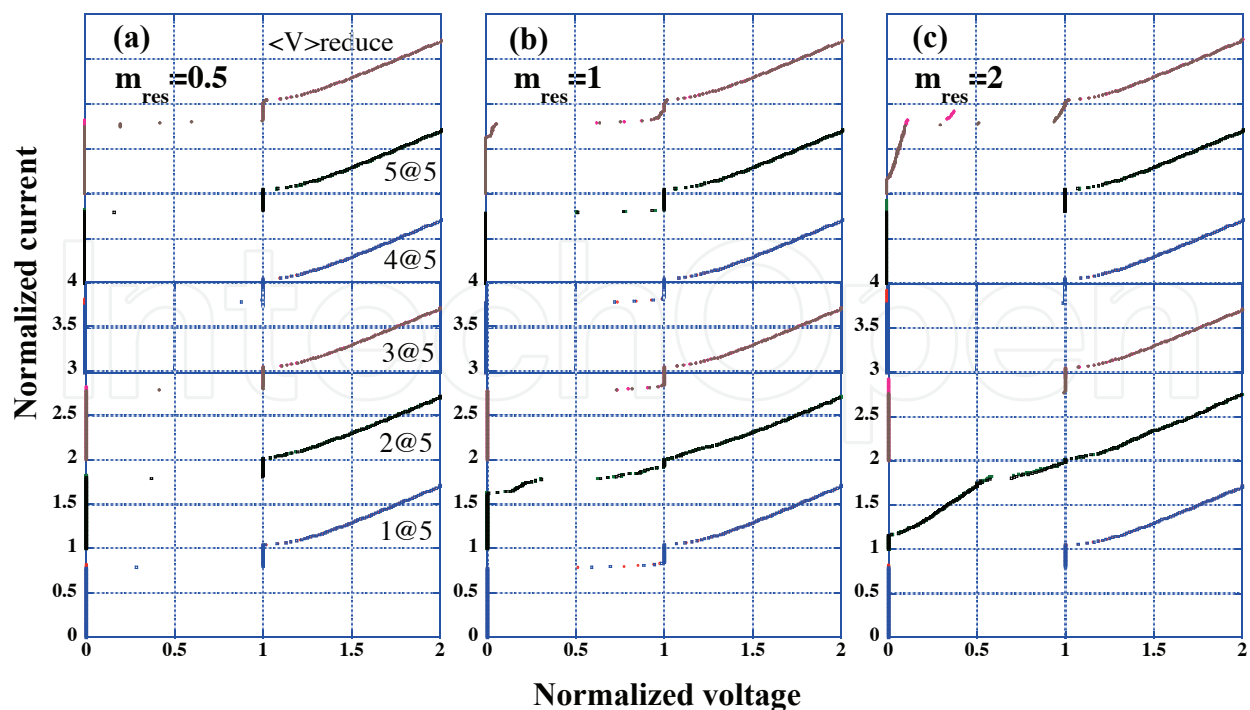
Fig. 6. The same as in Fig.5 but for $\Gamma = (0, m_{res}, 0, 0, 0)$, that is, the I-layer in 2@5 intermediate SIS junction is replaced by a F-layer. Shapiro steps are clearly found except for the 2@5 intermediate junction when $m_{res} = 2$ shown in (c).

we consider only the central case with $m(0) = 0.5$. Namely, only an I-layer in the central SIS Josephson junction is replaced by a F-layer, therefore, the corresponding configuration Γ is $(0, 0, 0.5, 0, 0)$. The aim of the present section is to see the effect of $\chi_\ell(d_F)$ defined in Eq.(16) to the *I-V* characteristics.

The central case for $N = 5$ is considered so that the value of ℓ is 3. By using 0, 0.2, 0.4, 0.6 and 0.8 as a value of $\chi_3(d_F)$, I have calculated the *I-V* characteristics. The *I-V* characteristics calculated for $\chi_3(d_F) = 1.0, 0.8, 0.6, 0.4, 0.2$ and 0.0 are shown in Fig.10(a), (b), (c), (d), (e) and (f), respectively. Here note that from a symmetry consideration, only the *I-V* characteristics of 1@5-surface, 2@5-intermediate and 3@5-central junctions are shown in the respective figure. Figure 10 shows that (I) as is expected, the *I-V* characteristic of 3@5-central junction including F-layer surely changes due to the change of the value of $\chi_3(d_F)$, especially, the height of the Shapiro step decreases with the decreasing the $\chi_3(d_F)$ and reaches to zero when $\chi_3(d_F) = 0$, however, (II) those of 1@5-surface and 2@5-intermediate junctions without the F-layer fairly well remain the same for the changing the $\chi_3(d_F)$, and (III) clear Shapiro steps are found in 1@5-surface and 2@5-intermediate junctions irrespective of the value of $\chi_3(d_F)$. Equation (16) tells us that when $\chi_3(d_F) = 0$, the 3@5-central junction can be regarded as a simple non-superconducting RC-junction. This fact is clearly found in the *I-V* characteristic of 3@5-junction shown in (f), that is, in which a purely ohmic characterictic is found.

Next, let us consider the case of $\alpha \neq 0$ for the same calculation condition mentioned above. We consider again the central case with $m(\alpha) = 0.5$. As an example, we set the α to 1 so that the corresponding configuration Γ is $(1, 1, 1.5, 1, 1)$. The *I-V* characteristics calculated for $\chi_3(d_F) = 1.0, 0.8, 0.6, 0.4, 0.2$ and 0.0 are shown in Fig.11(a), (b), (c), (d), (e) and (f),
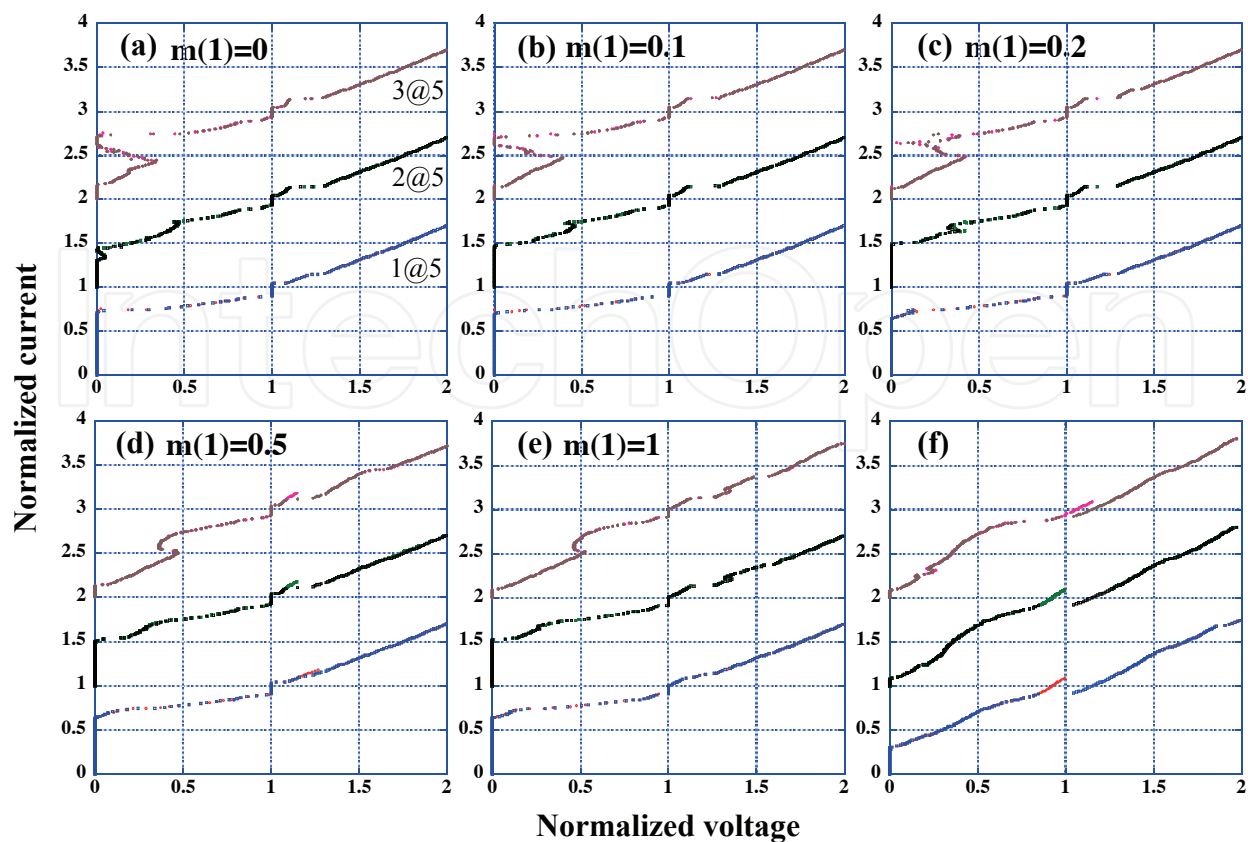
Fig. 7. The *I-V* characteristics of BSCCO IJJs calculated for $N = 5$, $J_c = 1000\text{A}/\text{cm}^2$, $f_p = 122\text{GHz}$, $f_r = 200\text{GHz}$, R_{shunt}/junction= 2Ω, SR_{shunt}/junction= $50\mu\text{m}^2\Omega$, $i_r = 1$, $L_x = 5\mu\text{m}$, i.e., $B_0(L_x) = 0.345\text{T}$ and $\chi_\ell(d_F) = 1$ for all junctions. The external magnetic induction B_{ext} is equal to $B_0(L_x)$ because of $\alpha = 1$. The I-layer in the 3@5 central SIS-Josephson junction is replaced by a F-layer so that the corresponding configuration $\boldsymbol{\Gamma}$ is $(1, 1, 1 + m(1), 1, 1)$. (a), (b), (c), (d) and (e) are for $m(1) = 0$, 0.1, 0.2, 0.5 and 1, respectively. For the comparison, the *I-V* characteristics calculated for $\boldsymbol{\Gamma} = (2, 2, 2, 2, 2)$ are also shown in (f). From the symmetry, only the *I-V* characteristics of 1@5 surface, 2@5 intermediate and 3@5 central junctions are shown. The horizontal axis indicates the dc voltage normalized to $\Phi_0 f_r$, and the vertical one shows the normalized dc i_0. (a) and (f) are equal to Fig.2(e) and (f), respectively. Shapiro steps are clearly found in all the *I-V* characteristics drawn in (a) to (e).

respectively. Figure 11 leads us a same conclusion mentioned above such that due to the decreasing the value of $\chi_3(d_F)$, (I) the *I-V* characteristic of 3@5 junction including the F-layer gradually changes, but those of 1@5 and 2@5 junctions without the F-layer well remain the same, and (II) Shapiro steps are clearly found in 1@5 and 2@5 junctions, but the height of the Shapiro step found in 3@5 junction decreases and reaches to zero when $\chi_3(d_F) = 0$.

From the above, we can say that the effect of $\chi_3(d_F)$ defined in the 3@5-central junction to the other junctions is negligible small irrespective of the value of the external magnetic field H_{ext}. This finding tells us that even if the BSCCO junction array with a multi-stacking structure is considered, the influence of the F-layer is restricted within a SFS-junction *itself*, i.e., that is negligible for others.
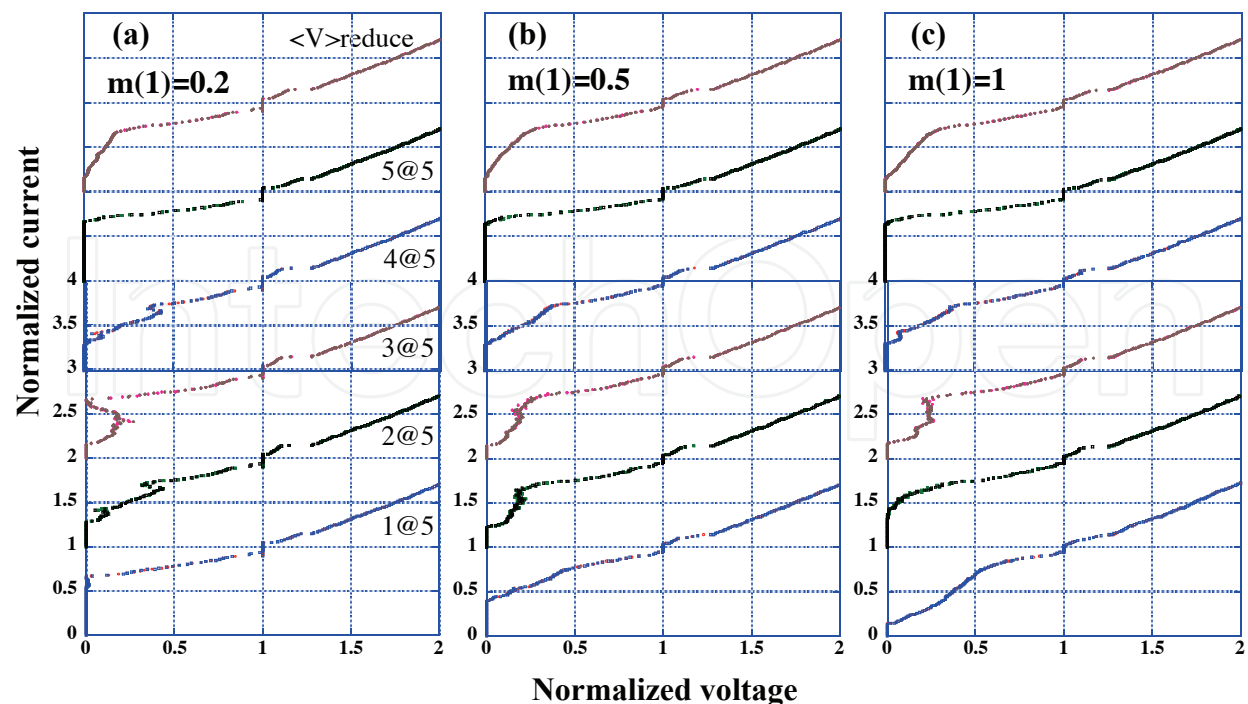
Fig. 8. The same as in Fig.7 but for the surface case, i.e., $\Gamma = (1 + m(1), 1, 1, 1, 1)$. The I-layer in 1@5 surface SIS junction is replaced by a F-layer so that the *I-V* characteristics of all junctions are shown together with the reduced voltage $< V >_{reduce}$. (a), (b) and (c) are for $m(1) = 0.2, 0.5$ and 1, respectively. The horizontal axis indicates the dc voltage normalized to $\Phi_0 f_r$, and the vertical one shows the normalized dc i_0. Shapiro steps are clearly found in all the *I-V* characteristics.

5. Summary

Shapiro steps in BSCCO IJJs have been studied full numerically. In the study, the *I-V* characteristics of not only the case of no external magnetic field but also the case in which an external magnetic field is applied parallel to the junction surface have been calculated by using the MS-unified theory including both the electric and magnetic field couplings between neighboring Josephson junctions.

For the effect of the junction length L_x along the x-axis, we have found that the overall profiles of the *I-V* characteristics including Shapiro steps calculated for the same external magnetic induction are fairly similar each other even if the junction length L_x differs each other.

For the effect of SR_{shunt}-product, we have found that it is essential to add the shunt resistance with a low-value into the BSCCO IJJs, if we wish to make a good quality Shapiro step device which is *hard* for the external magnetic disturbance. In the present study, therefore, the value of SR_{shunt}-product has been fixed to $50\mu\text{m}^2\Omega$/junction.

In order to see the effect of i_r to the *I-V* characteristics including Shapiro steps, I have calculated the *I-V* characteristics of nine cases such that $(i_r, \alpha) = (0, 0.5), (0, 1), (0, 2), (1, 0.5), (1, 1), (1, 2), (2, 0.5), (2, 1)$ and $(2, 2)$. Here note that the i_r is the normalized amplitude of the external ac modulation current with the frequency ω_r and the α defines the external magnetic induction B_{ext} as $\alpha B_0(L_x)$ using a constant magnetic induction $B_0(L_x)$. We have found that the
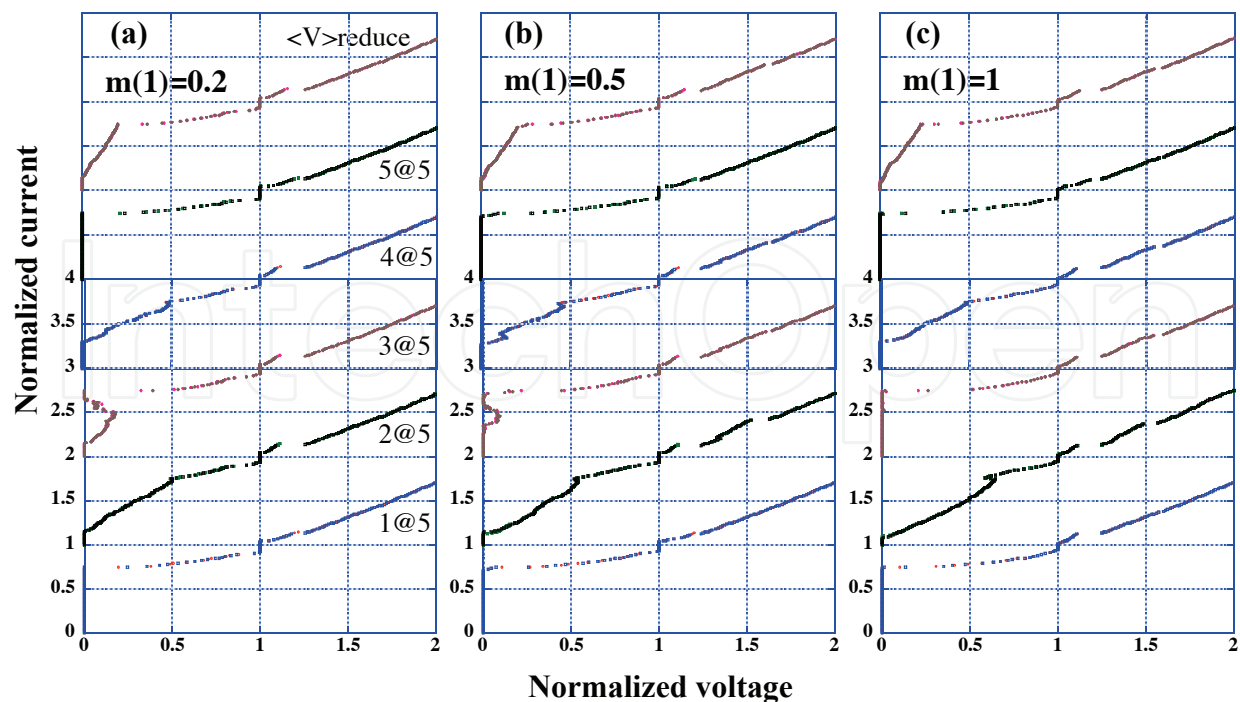
Fig. 9. The same as in Fig.7 but for the intermediate case, i.e., $\mathbf{\Gamma} = (1, 1 + m(1), 1, 1, 1)$. The I-layer in 2@5 intermediate SIS junction is replaced by a F-layer so that the *I-V* characteristics of all junctions are shown together with the reduced voltage $< V >_{reduce}$. (a), (b) and (c) are for $m(1) = 0.2, 0.5$ and 1, respectively. The horizontal axis indicates the dc voltage normalized to $\Phi_0 f_r$, and the vertical one shows the normalized dc i_0. Shapiro steps are clearly found in all the *I-V* characteristics.

Shapiro step and the flux flow could be treated separately under the presence of the external magnetic field.

From the *I-V* characteristics as a function of α, we have found that (I) the α-dependence of the normalized height $\Delta i_1(\alpha, N)$ of the 1st-order Shapiro step is very similar even if the N differs each other, however, (II) the α-dependence of the normalized critical current $i_c(\alpha, N)$ largely differs for $N = 1$ and 5, that is, the α-dependence of the $i_c(\alpha, N)$ is strongly affected by the magnetic interaction between neighboring Josephson junctions.

Within the framework of the MS-unified theory, I have studied the effect of ferromagnetic(F) layers into the *I-V* characteristics of BSCCO IJJs. In the present paper, we have studied the simplest case such that only the ℓ-th insulating(I)-layer in the BSCCO-IJJs is replaced by a F-layer whose the value of the magnetization is $M(B_{ext})$ as a function of the external magnetic induction B_{ext}. The effect of the magnetic field is taken into account via the boundary condition at the junction edge, so that the effective magnetic induction $B_{eff}^{(j)}$ at the edge of the j-th IJJ is given by $B_{ext} + M(B_{ext})\delta_{j,\ell}$. We have found that when $B_{ext} = 0$, (I) Shapiro steps are clearly found except for the junction including F-layer with a large residual magnetization $M_{res} \equiv m_{res}B_0(L_x)$ such as $m_{res} = 2$, (II) the *I-V* characteristics of the junction including F-layer are gradually changed due to the increasing the value of m_{res}, but (III) no remarkable change is found for the other junctions without F-layer. For $B_{ext} \neq 0$, i.e., $\alpha \neq 0$, in which the magnetization $M(B_{ext})$ is written as $m(\alpha)B_0(L_x)$, we have found that (IV) even in the
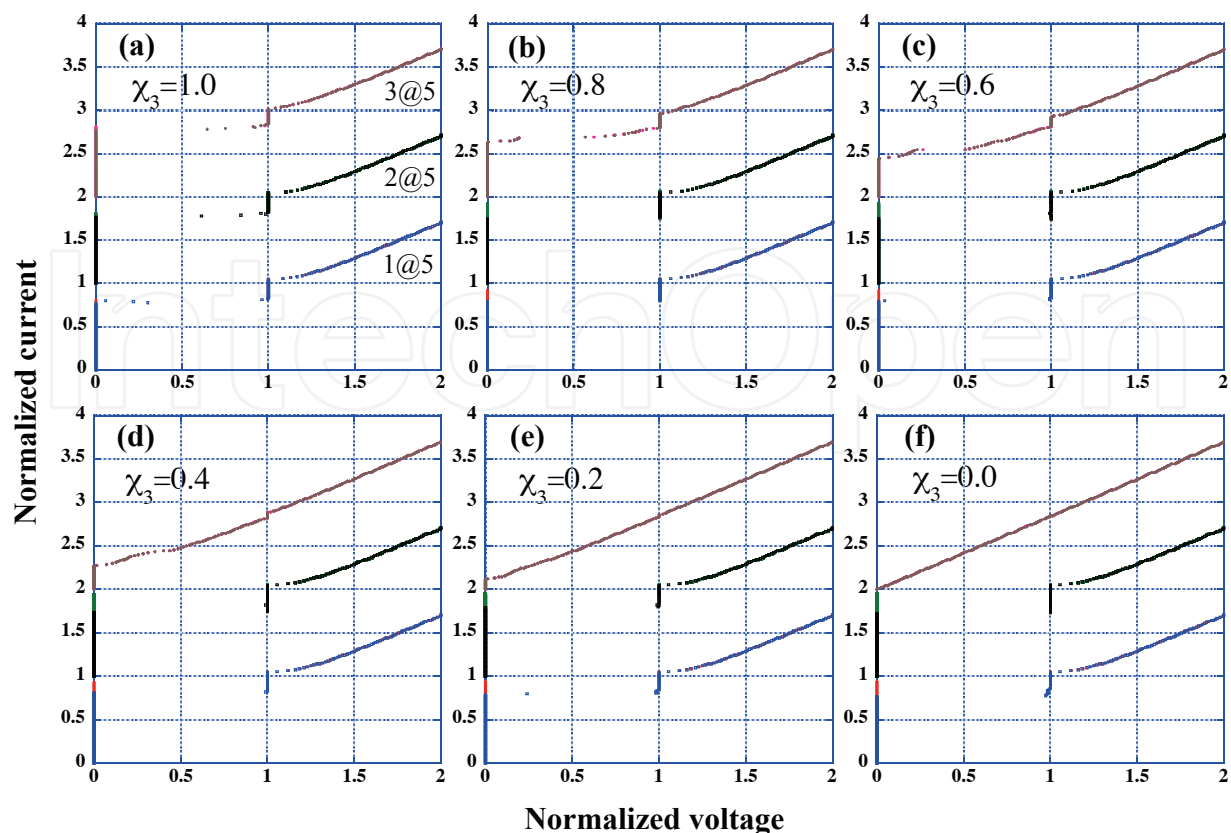
Fig. 10. The I-V characteristics of BSCCO IJJs calculated for $N = 5$, $J_c = 1000 \text{A/cm}^2$, $f_p = 122\text{GHz}$, $f_r = 200\text{GHz}$, R_{shunt}/junction$= 2\Omega$, SR_{shunt}/junction$= 50\mu\text{m}^2\Omega$, $i_r = 1$, $L_x = 5\mu\text{m}$, i.e., $B_0(L_x) = 0.345\text{T}$. In this figure, the central case has been considered and the configuration $\mathbf{\Gamma}$ has been tentatively selected as $(0, 0, 0.5, 0, 0)$. For the $\chi_\ell(d_F)$ defined in Eq.(16), only the value for $\ell = 3$ has been corrected, i.e., that of others has been held to 1. The value of $\chi_3(d_F)$ is 1.0, 0.8, 0.6, 0.4, 0.2 and 0.0 for (a), (b), (c), (d), (e) and (f), respectively. From the symmetry, only the I-V characteristics of 1@5 surface, 2@5 intermediate and 3@5 central junctions are shown. The horizontal axis indicates the dc voltage normalized to $\Phi_0 f_r$, and the vertical one shows the normalized dc i_0. Note that (a) is equal to Fig.4(d).

case of $\alpha \neq 0$, the findings (II) and (III) mentioned above are basically held again, but for the finging (I) we have found that (V) clear Shapiro steps are found in not only the junction without F-layer but also the junction including F-layer. In addition to the above calculations, I have further calculated the I-V characteristics for the surface and intermediate cases when $\alpha = 1$, whose the configurations are $(1 + m(1), 1, 1, 1, 1)$ and $(1, 1 + m(1), 1, 1, 1)$, respectively. We have concluded that even in the case in which a junction in BSCCO IJJs includes a F-layer with a finite magnetization, (I) the effect of the magnetic interaction between neighboring junctions is not so clearly found when $B_{ext} = 0$, but (II) when $B_{ext} \neq 0$, that is found clearly. Conclusion (II) obtained here is the same as a previous statement such that in the BSCCO IJJs with a stacking structure, there are considerable magnetic interactions between neighboring Josephson junctions when $\alpha \neq 0$. [36]

In order to see the effect of the F-layer in the SFS-junction to the I-V characteristics of BSCCO IJJs with a stacking structure, I have calculated the I-V characteristics as a function of $\chi_\ell(d_F)$ defined in Eq.(16). From the results calculated for the no external magnetic field and the
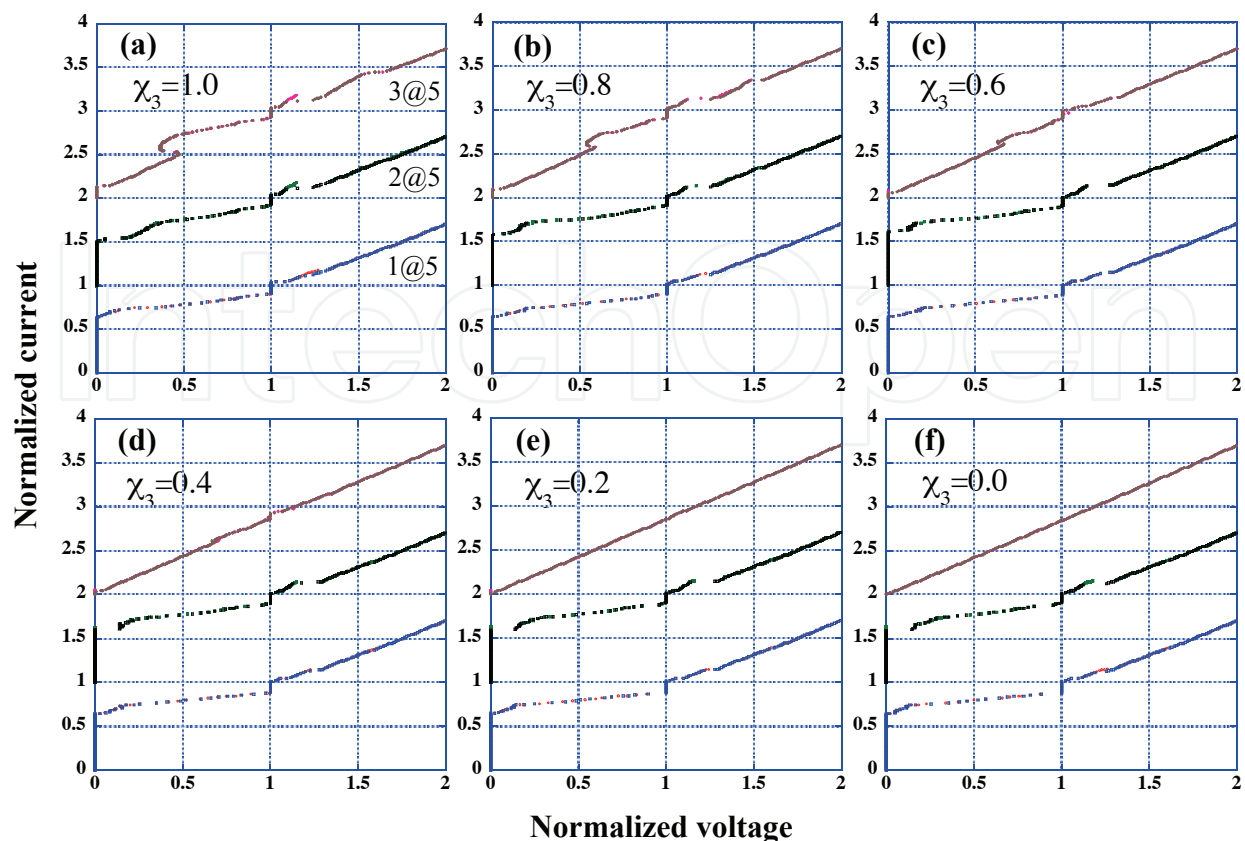
Fig. 11. The same as in Fig.10 but for the case of $\Gamma = (1, 1, 1.5, 1, 1)$. Note that (a) is equal to Fig.7(d).

nonzero field such as $\alpha = 0$ and 1, we have found that the effect of $\chi_3(d_F)$ defined in the 3@5-central junction to the other junctions is negligible small irrespective of the value of the external magnetic field H_{ext}, namely, the influence of the F-layer is restricted within a SFS-junction *itself*, i.e., that is negligible for others.

6. Acknowledgments

7. References

[1] S. Shapiro, Phys. Rev. Lett. 11, 80 (1963).
[2] R. Kleiner, F. Steinmeyer, G. Kunkel, and P. Müller, Phys. Rev. Lett. 68, 2394 (1992).
[3] G. Oya, N. Aoyama, A. Irie, S. Kishida, and H. Tokutaka, Jpn. J. Appl. Phys. 31, L829 (1992).
[4] R. Kleiner and P. Müller, Phys. Rev. B 49, 1327 (1994).
[5] A. Yurgens, D. Winkler, N. V. Zavaritsky, and T. Claeson, Phys. Rev. B 53, R8887 (1996).
[6] Yu. I. Latyshev, J. E. Nevelskaya and P. Monceau, Phys. Rev. Lett. 77, 932 (1996).
[7] K. Schlenga, R. Kleiner, G. Hechtfischer, M. Mößle, S. Schmitt, P. Müller, Ch. Helm, Ch. Preis, F. Forsthofer, J. Keller, H. L. Johnson, M. Veith, and E. Steinbeiß, Phys. Rev. B 57, 14518 (1998).

[8]   A. Irie, Y. Hirai, and G. Oya, Appl. Phys. Lett. 72, 2159 (1998).

[9]   D. J. Van. Harlingen, Rev. Mod. Phys. 67, 515 (1995).

[10] C. C. Tsuei and J. R. Kirtley, Rev. Mod. Phys. 72, 969 (2000).

[11] A. Damascelli, Z. Hussain, and Z. -X. Shen, Rev. Mod. Phys. 75, 473 (2003).

[12] Y. J. Doh, J. Kim, K. T. Kim, and H. J. Lee, Phys. Rev. B 61, R3834 (2000).

[13] H. B. Wang, P. H. Wu and T. Yamashita, Phys. Rev. Lett. 87, 107002 (2001).

[14] Yu. I. Latyshev, M. B. Gaifullin, T. Yamashita, M. Machida, and Y. Matsuda, Phys. Rev. Lett. 87, 247007 (2001).

[15] H. B. Wang, P. H. Wu, J. Chen, K. Maeda, and T. Yamashita, Appl. Phys. Lett. 80, 1604 (2002).

[16] G. Oya, A. Terada, N. Takahashi, A. Irie, and T. Hashimoto, Jpn. J. Appl. Phys. 44, L491 (2005).

[17] G. Oya, T. Hashimoto, and A. Irie, Supercond. Sci. Technol. 19, S191 (2006).

[18] H. B. Wang, S. M. Kim, S. Urayama, M. Nagao, T. Hatano, S. Arisawa, T. Yamashita, and P. H. Wu, Appl. Phys. Lett. 88, 063503 (2006).

[19] A. Barone and G. Paterno, *Physics and Applications of the Josephson Effect* (Wiley, New York, 1982).

[20] S. Sakai, P. Bodin, and N. F. Pedersen, J. Appl. Phys. 73, 2411 (1993).

[21] R. Kleiner, P. Müller, H. Kohlstedt, N. F. Pedersen, and S. Sakai, Phys. Rev. B 50, 3942 (1994).

[22] R. Kleiner, Phys. Rev. B 50, 6919 (1994).

[23] S. Sakai, A. V. Ustinov, H. Kohlstedt, A. Petraglia, and N. F. Pedersen, Phys. Rev. B 50, 12905 (1994).

[24] T. Koyama and M. Tachiki, Phys. Rev. B 54, 16183 (1996).

[25] V. M. Krasnov and D. Winkler, Phys. Rev. B 56, 9106 (1997).

[26] M. Machida, T. Koyama and M. Tachiki, Physica C 362, 16 (2001).

[27] A. E. Koshelev, Phys. Rev. B 66, 224514 (2002).

[28] M. Machida, Phys. Rev. Lett. 90, 037001 (2003).

[29] M. Machida and S. Sakai, Phys. Rev. B 70, 144520 (2004).

[30] A. V. Ustinov and N. F. Pedersen, Phys. Rev. B 72, 052502 (2005).

[31] S. Madsen and N. F. Pedersen, Phys. Rev. B 72, 134523 (2005).

[32] B. Y. Zhu, H. B. Wang, S. M. Kim, S. Urayama, T. Hatano, and X. Hu, Phys. Rev. B 72, 174514 (2005).

[33] M. Machida, Phys. Rev. Lett. 96, 097002 (2006).

[34] A. Irie and G. Oya, Supercond. Sci. Technol. 20, S18 (2007).

[35] M. Kitamura, A. Irie, and G. Oya, Phys. Rev. B 76, 064518 (2007).

[36] M. Kitamura, A. Irie, and G. Oya, J. Appl. Phys. 104, 063905 (2008).

[37] V. V. Ryazanov, V. A. Oboznov, A. Yu. Rusanov, A. V. Veretennikov, A. A. Golubov, and J. Aarts, Phys. Rev. Lett. 86, 2427 (2001).

[38] T. Kontos, M. Aprili, J. Lesueur, F. Genêt, B. Stephanidis, and R. Boursier, Phys. Rev. Lett. 89, 137007 (2002).

[39] A. A. Golubov, M. Yu. Kupriyanov, and E. Il'ichev, Rev. Mod. Phys. 76, 411 (2004).

[40] A. I. Buzdin, Rev. Mod. Phys. 77, 935 (2005).

[41] V. A. Oboznov, V. V. Bol'ginov, A. K. Feofanov, V. V. Ryazanov, and A. I. Buzdin, Phys. Rev. Lett. 96, 197003 (2006).

[42] J. W. A. Robinson, S. Piano, G. Burnell, C. Bell, and M. G. Blamire, Phys. Rev. Lett. 97, 177003 (2006).

[43] M. Weides, M. Kemmler, H. Kohlstedt, R. Waser, D. Koelle, R. Kleiner, and E. Goldobin, Phys. Rev. Lett. 97, 247001 (2006).

[44] S. Hikino, M. Mori, S. Takahashi, and S. Maekawa, J. Phys. Soc. Jpn. 77, 053707 (2008).

[45] R. L. Kautz and R. Monaco, J. Appl. Phys. 57, 875 (1985).

[46] M. Kitamura, A. Irie, and G. Oya, Phys. Rev. B 66, 054519 (2002).

[47] M. D. Fiske, Rev. Mod. Phys. 36, 221 (1964).

[48] V. M. Krasnov, N. Mros, A. Yurgens, and D. Winkler, Phys. Rev. B 59, 8463 (1999).
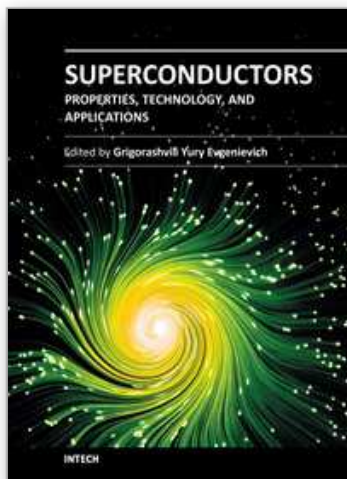
Superconductors - Properties, Technology, and Applications

Edited by Dr. Yury Grigorashvili

Book "Superconductors - Properties, Technology, and Applications" gives an overview of major problems encountered in this field of study. Most of the material presented in this book is the result of authors' own research that has been carried out over a long period of time. A number of chapters thoroughly describe the fundamental electrical and structural properties of the superconductors as well as the methods researching those properties. The sourcebook comprehensively covers the advanced techniques and concepts of superconductivity. It's intended for a wide range of readers.

How to reference

In order to correctly reference this scholarly work, feel free to copy and paste the following:

Michihide Kitamura (2012). Shapiro Steps in BSCCO Intrinsic Josephson Junctions, Superconductors - Properties, Technology, and Applications, Dr. Yury Grigorashvili (Ed.), ISBN: 978-953-51-0545-9, InTech, Available from: http://www.intechopen.com/books/superconductors-properties-technology-and-applications/shapiro-steps-in-bscco-intrinsic-josephson-junctions

INTECH
open science | open minds